



Published in final edited form as:

*Am J Med Genet A*. 2023 October ; 191(10): 2508–2517. doi:10.1002/ajmg.a.63320.

## Heterozygous Variants in *TBCK* Cause a Mild Neurologic Syndrome in Humans and Mice

Divya Nair<sup>1,\*</sup>, Abdias Diaz-Rosado<sup>1,2,\*</sup>, Elisa Varella-Branco<sup>3,\*</sup>, Igor Ramos<sup>3</sup>, Aaron Black<sup>1</sup>, Rajesh Angireddy<sup>1</sup>, Joseph Park<sup>2</sup>, Svathi Murali<sup>1,4</sup>, Andrew Yoon<sup>1</sup>, Brianna Ciesielski<sup>5</sup>, W. Timothy O'Brien<sup>5</sup>, Maria Rita Passos-Bueno<sup>\*,5</sup>, Elizabeth Bhoj<sup>\*,1</sup>

<sup>1</sup>Department of Genetics, Children's Hospital of Philadelphia, Philadelphia, PA, 19104 USA

<sup>2</sup>Department of Physiology, University of Pennsylvania Perelman School of Medicine, Philadelphia, PA 19104, USA

<sup>3</sup>Centro de Estudos do Genoma Humano e Células-Tronco, Universidade de São Paulo, São Paulo, Brazil

<sup>4</sup>Department of Engineering, University of Pennsylvania, Philadelphia, PA 19104, USA

<sup>5</sup>ITMAT, University of Pennsylvania, School of Medicine, Philadelphia, PA, 19104 USA

### Abstract

TBCK-related encephalopathy is a rare pediatric neurodegenerative disorder caused by biallelic loss-of-function variants in the *TBCK* gene. After receiving anecdotal reports of neurologic phenotypes in both human and mouse *TBCK* heterozygotes, we quantified if *TBCK* haploinsufficiency causes a phenotype in mice and humans. Using the *tbck*<sup>+/-</sup> mouse model, we performed a battery of behavioral assays and mTOR pathway analysis to investigate potential alterations in neurophysiology. We conducted as well a PheWAS analysis in a large adult biobank to determine the presence of potential phenotypes associated to this variant. The *tbck*<sup>+/-</sup> mouse model demonstrates a reduction of exploratory behavior in animals with significant sex and genotype interactions. The concurrent PheWAS analysis of 10,900 unrelated individuals showed that patients with one copy of a *TBCK* loss-of-function allele had a significantly higher rate of acquired toe and foot deformities, likely indicative of a mild peripheral neuropathy phenotype. This study presents an example of what may be the underappreciated occurrence of mild neurogenic symptoms in heterozygote individuals of recessive neurogenetic syndromes.

\*Corresponding author: bhoje@chop.edu.

\*These authors contributed equally to this work

Author roles: Data collection was performed by DN, ADR, AB, RA, JP, SM, AY, BC, EVB, IR MRPB. Experimental design was performed by DM, ADR, JP, WTB, EB, EVB, IR, MRPB. Manuscript writing was performed by ADR, AB, JP, SM, AY, EVB, IR, MRPB.

Conflict of interest disclosure – No authors have a conflict of interest.

Ethics approval statement – This work was approved by the IRB at University of Pennsylvania and the IACUC at Children's Hospital of Philadelphia.

Patient consent statement – No individual patient information is included in the report.

Permission to reproduce material from other sources – There is no material from other sources.

Clinical trial registration – This work does not include a clinical trial.

Ethics Declaration: The study was approved by the Institutional Review Board of the University of Pennsylvania and complied with the principles set out in the Declaration of Helsinki.

## Introduction:

Biallelic loss of function (LOF) variants in the *TBCK* gene cause TBCK-related encephalopathy (TBCKE), an autosomal recessive disorder with recognizable intellectual disability and hypotonia affecting both the central and peripheral nervous system. Affected individuals typically present with progressive neurologic dysfunction due to brain atrophy, frequently with concomitant neuromuscular weakness, coarse facies, and chronic respiratory failure<sup>1-4</sup>. Individuals with severe disease usually die before the third decade of life due to respiratory complications. Although there is significant variability within the syndrome, evidence for a genotype-phenotype correlation has been observed. There are currently no targeted treatments for this disorder and no description of the phenotypes of the heterozygotes of *TBCK* variants have been published.

TBCK protein contains three different functional domains, an N-terminal serine/threonine kinase domain, central Tre-2/Bub2/Cdc16 (TBC) domain, and a C-terminal rhodanese homology domain (RHOD). It was recently found that TBCK makes up one of the five parts of the Five-subunit Endosomal Rab5 and RNA/ribosome intermediarY (FERRY) complex, which transports mRNA within the cell for local translation. Specifically, it was shown to be vital for the transport of nuclear mRNA encoding mitochondrial proteins. FERRY interacts with Rab5, and it is speculated that the TBC domain of TBCK could act as a Rab GTP-hydrolysis activating protein (GAP), catalyzing GTP hydrolysis of Rab GTPases<sup>5, 6</sup>. In silico analysis suggests the kinase domain is not catalytically active, and very little is known about the RHOD domain<sup>1</sup>. Although there is no direct evidence of TBC domain activity, multiple missense variants in this region can cause an array of neurologic symptoms in affected individuals, indicating the critical role of this domain in TBCK protein function<sup>1; 2; 7</sup>.

Studies from patient-derived and TBCK knock-down (KD) cells of different types (such as fibroblasts, neuroprogenitor patient cells) show that TBCK deficiency downregulates mTOR signaling, affecting critical cellular processes like cell growth, proliferation, migration, cell division, and autophagy.<sup>1,3,8</sup> Aberrant mTORC1 signaling is observed in several autism-related syndromes, including tuberous sclerosis complex (TSC), Rett syndrome (RTT), Angelman syndrome, and neurofibromatosis type 1 (NF1), which are characterized by impairments in social interaction, communication, and other atypical behavior patterns<sup>9</sup>. While many of these disorders exhibit increased mTORC1 activity in patient-derived cells and brain tissues, a human pluripotent stem cell model of RTT shows decreased mTORC1 signaling. These findings suggest that bidirectional deviation in mTORC1 signaling can affect social behavior and cognition<sup>9</sup>. Similarly, mTORC1 suppression in cerebellar Purkinje cells negatively affects social interaction in mice<sup>10</sup>, highlighting that dysregulated mTORC1 signaling in the mouse brain can affect behavioral change. TBCK patient-derived fibroblasts harboring a p.R126X variant display mitochondrial respiratory defects, increased mitophagy, and supranormal accumulation of autophagosomes<sup>3</sup>. Treatment with acidifying lysosomal nanoparticles alleviated the mitochondrial respiratory defects, indicating that dysfunction in the autophagy-lysosomal pathway may play a critical role in TBCKE pathogenesis. Insufficient clearance of autophagosomes has been implicated in multiple

neurodegenerative disorders, including Parkinson's and Huntington's disease.<sup>3, 11</sup> Impaired vesicle trafficking from the endoplasmic reticulum to Golgi also seems to be impaired in neuroprogenitor cells (iNPCs) derived from induced pluripotent stem cells of TBCKE patients.<sup>27</sup>

While the mechanism of disease has yet to be determined, biallelic *TBCK* LOF results in severe neurogenic disease with both CNS and neuromuscular components. During the process of establishing a *TBCK* KO mouse colony, our lab anecdotally observed abnormal behavior in heterozygous animals, leading us to suspect that *TBCK* LOF may present with a haploinsufficiency phenotype in mice. In order to investigate this hypothesis, we performed a battery of behavior assays in a *TBCK*<sup>+/-</sup> mouse model, as well as examined mTOR signaling pathway modulation in the brain. Contemporaneously, patient families reported to us that the "unaffected" heterozygotes of TBCKE seemed to have mild neurologic findings, most closely resembling apraxia. Therefore, we also conducted a human phenome-wide association study (PheWAS) of 10,900 unrelated individuals from the Penn Medicine Biobank (PMBB), with the goal of identifying phenotypes which significantly correlate with heterozygote status for predictive loss-of-function (pLOF) *TBCK* variants.

## Materials and Methods:

### Phenome-Wide Association Studies – PheWAS Penn Medicine BioBank:

All individuals who were recruited for the Penn Medicine BioBank (PMBB) are patients of clinical practice sites of the University of Pennsylvania Health System. Appropriate consent was obtained from each participant regarding storage of biological specimens, genetic sequencing, access to all available electronic health record (EHR) data, and permission to recontact for future studies. The study was approved by the Institutional Review Board of the University of Pennsylvania and complied with the principles set out in the Declaration of Helsinki.

### Whole-exome sequencing and variant annotation:

This study included a subset of 11,451 individuals in the PMBB who have undergone whole-exome sequencing (WES). For each individual, we extracted DNA from stored buffy coats and then obtained exome sequences generated by the Regeneron Genetics Center (Tarrytown, NY), and these sequences were mapped to GRCh37. As previously described<sup>12</sup>, we removed samples with low exome sequencing coverage, high missingness, high heterozygosity, dissimilar reported and genetically determined sex, genetic evidence of sample duplication, and cryptic relatedness (*i.e.* 2<sup>nd</sup> degree or closer), leading to a total of 10,900 individuals for analysis. From the WES data, frameshift insertions/deletions, gain of stop codon variants, or variants disrupting canonical splice site dinucleotides in the *TBCK* gene were annotated as pLOF according to the NCBI Reference Sequence (RefSeq)<sup>13</sup> database via ANNOVAR (version 2018Apr16)<sup>14</sup>. For splicing variants, we removed those with SpliceAI scores < 0.2 for loss or gain of acceptor or donor site<sup>15</sup>.

**Clinical data collection:**

As previously described<sup>12</sup>, International Classification of Diseases Ninth Revision (ICD-9) and Tenth Revision (ICD-10) disease diagnosis codes and procedural billing codes, medications, and clinical imaging and laboratory measurements were extracted from the patients' EHR for PMBB. ICD-10 encounter diagnoses were mapped to ICD-9 via the Center for Medicare and Medicaid Services 2017 General Equivalency Mappings (<https://www.cms.gov/Medicare/Coding/ICD10/2017-ICD-10-CM-and-GEMs.html>) and manual curation. Phenotypes for each individual were then determined by mapping ICD-9 codes to distinct disease entities (*i.e.* Phecodes) via Phecode Map 1.2 using the R package "PheWAS"<sup>16</sup>. Patients were determined to have a certain disease phenotype if they had the corresponding ICD diagnosis on two or more dates, while phenotypic controls consisted of individuals who never had the ICD code. Individuals with an ICD diagnosis on only one date as well as individuals under control exclusion criteria based on PheWAS phenotype mapping protocols were not considered in statistical analyses.

**Association studies:**

A phenome-wide association study (PheWAS) approach was used to determine the phenotypes associated with TBCK pLOF variants carried by individuals in PMBB<sup>17</sup>. Each disease phenotype was tested for association with each gene burden or single variant using a logistic regression model adjusted for age, sex, and the first ten principal components (PCs) of genetic ancestry. We used an additive genetic model to collapse variants per gene via the fixed threshold approach<sup>18</sup>. Given the high percentage of individuals of African ancestry present in the discovery PMBB cohort, association analyses were performed separately in European (N=8,198) and African (N=2,172) genetic ancestries and combined with inverse variance weighted meta-analysis. Our association analyses considered only disease phenotypes with at least 20 cases, leading to the interrogation of 1,000 total Phecodes and a phenome-wide significance threshold of  $p=0.05/1000=5E-05$  to account for multiple testing with Bonferonni correction. All association analyses were completed using R version 3.3.5 (Vienna, Austria).

**Behavior:**

All animals were cared for in accordance with the ethical guidelines of the National Institutes of Health. The University of Pennsylvania Institutional Animal Care and Use Committees approved all animal procedures. All mouse lines were acquired from the Jackson Laboratory. The TBCK KO line (TBC1 domain containing kinase; targeted mutation 1b, Helmholtz Zentrum Muenchen GmbH), was backcrossed to C57BL/6J for six generations to generate the mice used in this study.

**Elevated Zero Maze:**

Exploration of the elevated zero maze is sensitive to anxiolytic drugs thus, it is used routinely to assess anxiety-related behavior. The maze consists of a 2" wide circular track with two walled and two open areas, elevated 16" above the floor. Mice were habituated to the procedure room for 30 minutes prior to the test. A 5-minute trial began with a mouse placed in the center of a walled area. Digitally recorded trials were processed for automated

analysis by ANYmaze software (Stoelting Co) to generate the time spent in the open areas of the maze and distance traveled.

### **Open Field Activity:**

Spontaneous activity in an open field arena is commonly used to assess locomotion and rearing. A Photobeam Activity System (San Diego Instruments) was used to acquire data. The clear Plexiglas arena (16 in. x 16 in. x 18 in.) is fitted with IR emitters and photo sensors to detect beam breaks as peripheral, center and rearing activity. After a 30-minute habituation to the testing room, a 10-minute trial began with a mouse placed in the center of the arena.

### **Accelerating Rotarod:**

The Rotarod (IITC San Diego Ca.) is a 1” diameter, horizontal rod with a knurled surface, programmable to accelerate at different rates. As the rod accelerates, the mouse must adjust the cadence of its stride to remain on the rod. The mouse was lowered gently onto the stationary rod and then rotation was started. A trial ends when the mouse fails to walk, by either falling from the rod or making a full rotation while gripping the rod. Mice that completed the full 300 seconds were removed from the rod to end the trial. A modified high-speed protocol was employed to assess repetitive motor behavior<sup>19</sup>. Each day, prior to the test, mice were habituated to the procedure room for thirty minutes. Mice received three trials per day, with an intertrial interval of 30 minutes, over four consecutive days. On the first two days, the rotarod accelerated from 4 to 40 rpm; on the last two days, the rotarod accelerated from 8 to 80 rpm. Between all trials, the equipment was wiped with 70% EtOH. On the first trial only, mice were placed on the stationary rod for two minutes for habituation before acceleration began. The latency to failure to continue walking was noted.

### **Spontaneous Alternations in a Y-maze:**

During exploration of a three-armed maze, mice demonstrate an innate propensity to avoid entering the “just-visited” arm, with preference for the arm not “just-visited”. Thus, in a Y shaped maze, with arms designated A, B and C, mice stereotypically travel from arm A to B to C then back to A, spontaneously alternating the sequence of arms entered. Departure from this strategy, for example from A to B to A suggests a failure to recall exploration of the “just-visited” arm and is indicative of a short term or working memory impairment. After 30 minutes of habituation to the procedure room, a mouse was placed at the end of an arm and allowed to explore freely for 8 minutes. A Y-maze with 15” long x 3” wide arms (San Diego Instruments) was used. High-definition video recordings were for graded by an individual blind to group designation. Entry into an arm was defined as when all four paws were placed inside an arm. The percent spontaneous alternation was calculated as  $100 \times [\text{number of alterations} / (\text{total arm entries} - 2)]$ . The total number of arm entries is also determined as a measure of activity.

### **Acoustic Startle Response and Pre-pulse inhibition:**

The acoustic startle response (ASR) procedure assesses reactivity to audible stimuli. Mice were tested with the SR-Lab system (San Diego Instruments). Mice were placed in a 5”

x 1.75" dia. tube mounted on a platform with a stabilimeter, within a sound attenuating cabinet. The movement of the mouse was detected as a voltage disruption by the stabilimeter and transduced to a digital format. Motion was sampled for 120 msec after each stimuli presentation. A small speaker mounted inside the cabinet delivered the stimuli. A continuous 70dB white noise background was presented throughout the session. After a 5 min acclimation to the background noise, the mice received a block of 40 msec, 120dB white noise bursts to collect baseline reactivity. This was immediately followed by a block of white noise bursts (100,110,120 dB and background noise) randomly delivered, 8–15 sec. apart. Each intensity was presented 6 times in a pseudo-randomized fashion. Peak amplitude of the startle response, average response, total movement during the trial and latency to peak startle response were acquired. The data were used to calculate an intensity-response curve.

Pre-pulse inhibition (PPI) trials followed the intensity-response block of trials. PPI naturally occurs when a weaker, non-startle evoking stimulus precedes a stronger startle-evoking stimulus. The pre-pulse stimuli is predictive of the higher intensity stimuli so that the typical response to the startle-evoking stimuli is attenuated. A disruption of the inhibition suggests a sensory-motor response integration deficit. The 120 dB startle-evoking stimuli were delivered either alone (no pre-pulse) or preceded by a 20 msec pre-pulse, delivered at three different intensities (78, 81 or 85 dB). PPI for each pre-pulse intensity is calculated as the percent decrease of the pre-pulse startle responses compared to no-prepulse responses. An assessment of habituation is also obtained by comparing responses to a final block of 6, 120dB stimuli to the responses of the first block of 120dB stimuli. Habituation is calculated as the percent reduction of the latter block relative to the former.

#### **Western blot:**

Brains from 14–16-week-old C57BL/6J mice were harvested, and total tissue lysates were prepared by homogenizing brain tissue in RIPA lysis buffer (0.1% SDS, 1% NP40 and 0.5% deoxycholate) with protease (cat#: 11873580001, Sigma-Aldrich) and phosphatase (cat#: 04906845001, Sigma-Aldrich) inhibitors. Protein concentration from total tissue lysates was estimated using the BCA Protein Assay kit (cat#: 23225, Thermo Scientific). A total of 30µg protein was separated by SDS-PAGE and transferred to PVDF membranes (cat#: IPVH00010, EMD Millipore). Western blotting is performed using primary antibodies to TBCK (cat#: HPA039951, Sigma), S6 (cat#: 37174, CST), phospho-S6 (cat#: 37174, CST), LC3 (cat#: L8918, Sigma), β-actin (cat#: Sc-69873, CST), and the blots were developed by incubating with ECL reagent (cat#: 34578, Thermo Scientific) and imaged in ChemiDoc (BioRad).

#### **Neurite dynamics assay:**

Neurons (50 days post neural induction) derived from control (n = 1), patient (n= 2) and heterozygote (n = 1) individuals were dissociated and plated on polyornithine and laminin coated 24-well clear plates (Corning® Costar® TC-Treated, CLS3527) at ~120,000 cells/mL. Plates were cultured, imaged and analyzed with the IncuCyte Live Cell Analysis System (Essen Bioscience) for 95h. Phase-contrast images were obtained at 20× magnification using the IncuCyte® system (Essen Bioscience). The Incucyte Neurotrack software module automatically processes the images and analyzes neurite dynamics. The cells were imaged

every 30 minutes with the IncuCyte System and the morphological parameters (cell body cluster area, neurite length and branch point number) were quantified. We selected five timepoints (2h, 24h, 48h, 72h, 95h) to observe the possible difference among groups. Each experimental condition was performed in 3 replicate wells. Patients' measures were merged and the mean was utilized in graphs. Data were normalized to control  $t = 2h$ , similarly to Srikanth et al. (2018)<sup>23</sup>.

### Statistics:

Two-way analysis of variance (ANOVA) was used to compare data for the open field (horizontal activity, rearings, center activity, and total activity), Y-maze (% spontaneous alternations and arm entries), elevated zero maze (time in open and distance traveled), and acoustic startle response (ASR) pre-pulse inhibition outcomes. These models assessed for differences in genotype, sex, and the genotype by sex interaction. For the rotarod data, repeated measures ANOVA, stratified by sex, was used to assess differences by trial, genotype, and genotype by trial interaction. Similarly, for the acoustic startle input/output response, repeated measures ANOVA, stratified by sex, was used to assess differences by intensity, genotype, and genotype by intensity interaction. Since the input/output response distribution was right-skewed, a log transformation was used to obtain approximately normal distributions. The models were run using the original, untransformed data and the log transformed data. Only the results of the original data are presented since the conclusions did not differ when using the log transformed data. Quantitative data are presented in the figures as means  $\pm$  standard error of the mean (SEM). Analyses were performed using SAS version 9.4 (SAS Institute, Cary, NC). For the neurite dynamics analysis, we performed a two-way ANOVA corrected for multiple comparisons with the Holm-Šidák test using GraphPad Prism 9 software.

### Results:

#### **PheWAS analysis shows that TBCK heterozygote status is significantly associated with acquired foot deformities**

In coordination with the PMBB, we assessed a sample of 10,900 unrelated individuals for TBCK pLOF gene burden. A total of 19 *TBCK*<sup>+/-</sup> heterozygotes were identified in this subset, representing 16 unique pLOF variants in *TBCK*. These variants were composed of seven frameshift insertions/deletions, five stop-gain variants, and four splicing variants disrupting canonical splice site dinucleotides. A PheWAS of the gene burden of pLOF variants in *TBCK* showed genome-wide significant associations with acquired hammer toe ( $p=4.39E-07$ ) and other acquired toe deformities ( $p=1.24E-06$ ), as well as near-significant associations with hallux valgus ( $p=2.59E-04$ ) and acquired foot deformities ( $p=4.62E-04$ ) (Figure 1). The subsequent review of significant phenotypes showed that 2 of 19 heterozygous individuals were diagnosed with both hammer toe and hallux valgus, phenotypes that are often the first signs of peripheral neuropathy. These results indicate that *TBCK* heterozygotes are predisposed to foot and toe deformities, likely due to peripheral neuropathy.

It is worth mentioning that, despite the differences observed in the *PheWAS* data, one limitation of this study lies in the lack of qualitative/phenotypic data obtained from a natural history study. Even though the genotype for many of these carriers have been molecularly confirmed, time constraints and availability of resources limited our ability to collect detailed information on the clinical presentation of these subjects. Nonetheless, shared anecdotes from informal conversations with family members led to the pursuit a phenotypic assessment in TBCK carrier, and hence a *PheWAS*.

### Behavioral studies show significant reductions in exploration drive for *TBCK*<sup>+/-</sup> animals

In the process of backcrossing our TBCK KO line to the C57BL/6J background, we found that the *TBCK*<sup>-/-</sup> genotype, which on the prior genetic background resulted in pre-weaning death, was now embryonic lethal. Furthermore, we soon observed an anecdotal pattern of abnormal behavior in our *TBCK*<sup>+/-</sup> mice. Based upon these findings, we chose to perform an in depth battery of behavioral assays to verify and investigate these abnormalities. Open field (OF) activity assays are commonly utilized to examine locomotor, exploratory, and anxiety-like behavior in mice<sup>20</sup>. WT and *TBCK*<sup>+/-</sup> mice were assayed for spontaneous open field activity over a 10-minute period. While no significant genotype-correlated difference was observed for horizontal, center, or total activity, we found that *TBCK*<sup>+/-</sup> group had significantly reduced rearing compared to WT ( $p = 0.0199$ ) (Figure 2A, B, C, D). Within the composite sex *TBCK*<sup>+/-</sup> group, there was also a sex-based difference, with only male *TBCK*<sup>+/-</sup> mice displaying a significant reduction in rearing (data not shown,  $p = 0.0324$ ). An accelerating rotarod assay did not elicit differences between *TBCK*<sup>+/-</sup> and WT animals, indicating that they likely do not suffer from balance or motor coordination defects (Figure 2E).

The acoustic startle response (ASR) measures the amplitude of the reflexive response to a loud acoustic stimulus. This response is mediated by a simple neural circuit located in the lower brain stem. The startle response can vary due to direct perturbations of this circuit, but can also be affected by other external and internal factors, including illumination, pharmacological compounds, anxiety, and neuropsychiatric disorders<sup>22</sup>. ASR is frequently used to evaluate if conditions or stimuli perturb sensorimotor integration. We performed ASR with startle evoking white-noise bursts of 100, 110, and 120dB. The overall *TBCK*<sup>+/-</sup> group did not show a significant difference in response compared to the WT group (data not shown). However, segregating the groups by sex revealed that female *TBCK*<sup>+/-</sup> mice responded less to stimuli of increasing decibels than WT females ( $p = 0.0155$ ) (Figure 2F). Pre-pulse inhibition (PPI) measures the attenuation of the acoustic startle response when it is preceded by a startle provoking sound of lower dB. It is used to examine sensorimotor gating, that is, the ability to attend to a predictive stimulus and modulate a response. Neuropsychiatric disorders with PPI dysfunction include attention deficit disorder, schizophrenia, Huntington's disease, and Tourette's syndrome<sup>22</sup>. *TBCK*<sup>+/-</sup> mice showed significant disruption of PPI at the 87-decibel pre-pulse stimulus as compared with WT mice ( $p = 0.0259$ ) (Figure 2G). No differences were observed at the 78 and 81-decibel pre-pulse stimuli. This reduction in PPI may represent a deficit in attention, wherein the animals are not able to properly process the pre-pulse stimulus.

The Y maze behavioral assay is used to assess working spatial memory in animals. We found that the number of spontaneous arm alternations observed did not change between WT and *TBCK*<sup>+/-</sup> animals at 3, 5, or 8 minutes, but that there was a significant reduction in the total number of arm entries at 8 minutes for *TBCK*<sup>+/-</sup> males as compared to WT males ( $p = 0.0449$ ) (Figure 3A & B). Reductions in the total number of arm entries can be attributed to impaired spontaneous locomotor activity or reduced exploratory behavior. However, our OF and rotarod data showed no reduction in motor function, suggesting that a reduction in exploratory drive is the likely cause. Mouse exploratory drive is often reduced in animals with anxiety-like behavior; to investigate if this is the case in *TBCK*<sup>+/-</sup> mice, we utilized the elevated zero maze (EZM) test, which quantifies the time the mice willingly spend in an exposed, stressful location<sup>21</sup>. These EZM results showed no differences in the time spent in open areas between *TBCK*<sup>+/-</sup> and WT mice, nor a significant difference in the distance traveled between groups. However, there was a statistically significant difference in distance traveled between male and female *TBCK*<sup>+/-</sup> mice ( $p = 0.0491$ ), with male heterozygotes traveling longer distances and female heterozygotes traveling shorter distances. This was largely driven by a strong trend toward less distance traveled in female *TBCK*<sup>+/-</sup> mice as compared to WT ( $p = 0.0703$ ) (Figure 3C & D). Typically, an increase in anxiety-like behavior would result in the mice spending less time in the open areas of the EZM, however we did not observe this. Instead, we found that female *TBCK*<sup>+/-</sup> mice traveled less than male *TBCK*<sup>+/-</sup>, and strongly trended towards less travel when compared to female WTs. These Y maze and EZM results suggest that while *TBCK*<sup>+/-</sup> mice do not show anxiety-related behavior, they may have reduced exploratory drive, resulting in reduced investigatory behavior.

Taken altogether, our behavioral results show that *TBCK*<sup>+/-</sup> animals present with a broad and subtle neurological phenotype, often with sex-dependent differences.

### **mTORC1 is differentially regulated in male vs female mice regardless of genotype**

Previous studies done in TBCK patient-derived fibroblast have revealed the significant impact that TBCK mutations can have upon mTOR signaling. Even though the mechanism is still unclear, recent studies have shown significant changes in autophagy and S6 phosphorylation<sup>1,3</sup>. Since both autophagy and phosphorylation of S6 are directly affected by mTOR signaling, we wished to determine whether our *TBCK*<sup>+/-</sup> mouse model would also display mTOR downregulation in CNS tissue. To investigate this, we performed WB analysis on WT and *TBCK*<sup>+/-</sup> total brain tissue lysates with antibodies to TBCK, total S6, phospho-S6, LC3, Phospho-p70 S6K, total p70 S6K, Phospho-4E-BP1 and total 4E-BP1. Unexpectedly, we observed no expression differences associated with genotype, but we did find that male mice, regardless of genotype, showed significant reductions in phospho-S6 (235/236) and p-4E-BP1 as compared to females (Figure 4A, C & E). As both phospho-S6 and p-4E-BP1 are direct readouts for mTORC1 activity, this indicates that mTORC1 signaling is reduced in male brains regardless of their genotype (Figure 4A, C & E). We did not observe any difference in the protein levels of TBCK, p-P70-S6K or autophagosomal marker LC3 (Figure 4A, B, D & F). These results indicate that, in general, mTOR signaling is differentially modulated in the brains of male and female mice. These

sex-based differences in mTOR signaling may explain why we often observe sex-based differences in *TBCK*<sup>+/-</sup> mouse behavior.

## Discussion

It is clear that there are shared mechanisms of pathology between rare neurogenetic disorders and common forms of similar diseases. In this study we wanted to investigate if TBCK-related encephalopathy (TBCKE), a severe autosomal recessive neurodegenerative disorder, also presents with a heretofore unrecognized mild form in *TBCK* heterozygotes. This was driven by unsolicited reports from families of children with TBCKE, describing mild neurodevelopmental differences in the heterozygous parents and siblings, most closely resembling non-specific apraxia. In parallel, during the expansion of our *TBCK* KO mouse colony we received multiple anecdotal reports that *TBCK*<sup>+/-</sup> mice displayed behavioral abnormalities when compared to WT littermates. Based upon these reports, we chose to quantify the neurobehavior differences in mice, and investigate the potential phenotypes in human heterozygotes through *PheWAS*.

To assess quantifiable neurobehavioral difference in the *TBCK*<sup>+/-</sup> mice, we performed a battery of behavior procedures. In summary, the results from these behavioral studies support the hypothesis that *TBCK*<sup>+/-</sup> mice evince less exploratory behavior than WT animals, often with sex-specific dimorphism. An open field activity assay did not show any significant differences for horizontal and center activity, but did show that heterozygous animals reared significantly less, with males more severely affected than females. The Y-maze assay found that male *TBCK*<sup>+/-</sup> mice entered new arms less frequently than WT males, while the elevated zero maze found that female *TBCK*<sup>+/-</sup> mice strongly trended towards traveling shorter distances in the assay ( $p = 0.0703$ ). This reduction in rearing and investigative behavior demonstrates diminished exploratory behavior among the *TBCK*<sup>+/-</sup> cohort. As TBCKE patients present both cognitive and neuromuscular defects, it was also necessary to distinguish between behavioral alterations caused by neurological changes and those potentially caused by reduced physical capabilities. In the *TBCK*<sup>+/-</sup> population, no differences were observed in the open field procedure for horizontal, center, and total activity, and the accelerating rotarod assay also did not uncover any abnormalities. Combined, these results suggest that any behavioral abnormalities identified are not driven by reduced physical function, and instead can be attributed to deficits in the specific behavior traits.

Interestingly, we also observed a striking sex difference in mTOR signaling in the brains of the heterozygote mice, but not a genotype-driven difference. As we didn't see a difference in TBCK protein levels between the heterozygous and wildtype littermates, it's possible that the WT allele is able to generate sufficient TBCK to maintain a generally normal homeostasis. In the future, it would be interesting to look at intracellular localization of TBCK protein, as well as examine the heterozygotes and wildtype littermates for other physiological and molecular differences that could explain their deviations in behavior. The sex difference in mTORC1 activation levels has been described previously in wildtype mice, with pS6 levels four times higher in fasted female mice<sup>26</sup>.

In a human PheWAS composed of >10,000 unrelated individuals, we found a phenome-wide significant correlation between TBCKE heterozygote status and both “acquired hammer toe” ( $p=4.39E-07$ ) and “other acquired toe deformities” ( $p=1.24E-06$ ). While puzzling at first, when the newly discovered role of TBCK in axonal mRNA transport was reported we were able to hypothesize that these phenotypes represent an axonal neuropathy presenting first with hammer toe, similar to Charcot-Marie-Tooth syndrome.<sup>24</sup> Since the autosomal recessive form of TBCKE is so clinically severe, we propose that a neuropathy would be overlooked. In this PheWAS we did not see any neurodevelopmental phenotypes, likely because we were limited to those diagnoses that are recorded in the adult electronic medical record (EMR.) Interestingly, a more severe muscular disease has been described in one family with biallelic *TBCK*LOF variants<sup>25</sup>. We hypothesize that milder learning disabilities or apraxias would not be recorded into the EMR in an adult-focused health system. We did attempt to perform a PheWAS in a pediatric biobank (Center for Applied Genomics at the Children’s Hospital of Philadelphia), but despite being the largest EMR-linked pediatric biobank, there were not enough patients with *TBCK*LOF variants within this smaller population to perform the analysis.

We would recommend that patients who are heterozygous for a pathogenic TBCK variant be evaluated in adulthood for signs of axonal neuropathy. Since our study included adult patients of all ages, some of whom may have yet to develop symptoms, we are unable to quantify the risk of neuropathy to an individual. We hope through dedicated genotyping and neurologic evaluation of *TBCK*LOF heterozygotes over time we will have the data to calculate this more specifically.

In conclusion, it is well-documented that autosomal recessive TBCK deficiency presents with a severe progressive neurodegenerative disorder. In this study we quantified the effects of heterozygosity for *TBCK*LOF in both humans and a mouse model. Utilizing PheWAS, we found a statistically significant correlation between *TBCK* heterozygosity and peripheral neuropathy, which is supported by recent cellular data showing the important role of TBCK in axonal mRNA trafficking. In addition, we saw decreased exploratory behavior in the TBCK heterozygous mice, suggesting a neurobehavior difference. Therefore, haploinsufficiency of TBCK results in a previously unidentified mild phenotype in both humans and mice. There are likely many other severe recessive disorders with overlooked mild phenotypes that can help explain some percentage of the incidence of common polygenic disorders.

## Funding statement –

We acknowledge funding from NIH/NINDS (K08NS109281). The Neurobehavior Testing Core at UPenn/ITMAT and IDDRRC at CHOP/Penn U54 HD086984 assisted with mouse behavior procedures. The Biostatistical Advisory Core at UPenn assisted with statistical analyses. We acknowledge the Regeneron Genetics Center for performing exome sequencing in participants in the Penn Medicine Biobank.

**This work was funded by NIH, NINDS K08NS109281to EJB.**

This work was funded by NIH, NINDS K08NS109281to EJB.

## Data Availability:

All variants described here are deposited in ClinVar. Any additional data will be provided upon request.

## References:

1. Bhoj EJ, Li D, Harr M, Edvardson S, Elpeleg O, Chisholm E, Juusola J, Douglas G, Guillen Sacoto MJ, Siquier-Pernet K, et al. (2016). Mutations in TBCK, Encoding TBC1-Domain-Containing Kinase, Lead to a Recognizable Syndrome of Intellectual Disability and Hypotonia. *Am J Hum Genet* 98, 782–788. [PubMed: 27040691]
2. Chong JX, Caputo V, Phelps IG, Stella L, Worgan L, Dempsey JC, Nguyen A, Leuzzi V, Webster R, Pizzuti A, et al. (2016). Recessive Inactivating Mutations in TBCK, Encoding a Rab GTPase-Activating Protein, Cause Severe Infantile Syndromic Encephalopathy. *Am J Hum Genet* 98, 772–781. [PubMed: 27040692]
3. Ortiz-Gonzalez XR, Tintos-Hernandez JA, Keller K, Li X, Foley AR, Bharucha-Goebel DX, Kessler SK, Yum SW, Crino PB, He M, et al. (2018). Homozygous boricua TBCK mutation causes neurodegeneration and aberrant autophagy. *Ann Neurol* 83, 153–165. [PubMed: 29283439]
4. Mandel H, Khayat M, Chervinsky E, Elpeleg O, and Shalev S (2017). TBCK-related intellectual disability syndrome: Case study of two patients. *Am J Med Genet A* 173, 491–494. [PubMed: 27748029]
5. Wu J, and Lu G (2021). Multiple functions of TBCK protein in neurodevelopment disorders and tumors. *Oncol Lett* 21, 17. [PubMed: 33240423]
6. Pan X, Eathiraj S, Munson M, and Lambright DG (2006). TBC-domain GAPs for Rab GTPases accelerate GTP hydrolysis by a dual-finger mechanism. *Nature* 442, 303–306. [PubMed: 16855591]
7. Hartley T, Wagner JD, Warman-Chardon J, Tetreault M, Brady L, Baker S, Tarnopolsky M, Bourque PR, Parboosingh JS, Smith C, et al. (2018). Whole-exome sequencing is a valuable diagnostic tool for inherited peripheral neuropathies: Outcomes from a cohort of 50 families. *Clin Genet* 93, 301–309. [PubMed: 28708278]
8. Liu Y, Yan X, and Zhou T (2013). TBCK influences cell proliferation, cell size and mTOR signaling pathway. *PLoS One* 8, e71349. [PubMed: 23977024]
9. Magdalon J, Sanchez-Sanchez SM, Griesi-Oliveira K, and Sertie AL (2017). Dysfunctional mTORC1 Signaling: A Convergent Mechanism between Syndromic and Nonsyndromic Forms of Autism Spectrum Disorder? *Int J Mol Sci* 18.
10. Sakai Y, Kassai H, Nakayama H, Fukaya M, Maeda T, Nakao K, Hashimoto K, Sakagami H, Kano M, and Aiba A (2019). Hyperactivation of mTORC1 disrupts cellular homeostasis in cerebellar Purkinje cells. *Sci Rep* 9, 2799. [PubMed: 30808980]
11. Tintos-Hernandez JA, Santana A, Keller KN, and Ortiz-Gonzalez XR (2021). Lysosomal dysfunction impairs mitochondrial quality control and is associated with neurodegeneration in TBCK encephaloneuronopathy. *Brain Commun* 3, fcab215. [PubMed: 34816123]
12. Park J, Lucas AM, Zhang X, Chaudhary K, Cho JH, Nadkarni G, Dobbyn A, Chittoor G, Josyula NS, Katz N, et al. (2021). Exome-wide evaluation of rare coding variants using electronic health records identifies new gene-phenotype associations. *Nat Med* 27, 66–72. [PubMed: 33432171]
13. O’Leary NA, Wright MW, Brister JR, Ciufu S, Haddad D, McVeigh R, Rajput B, Robbertse B, Smith-White B, Ako-Adjei D, et al. (2016). Reference sequence (RefSeq) database at NCBI: current status, taxonomic expansion, and functional annotation. *Nucleic Acids Res* 44, D733–745. [PubMed: 26553804]
14. Wang K, Li M, and Hakonarson H (2010). ANNOVAR: functional annotation of genetic variants from high-throughput sequencing data. *Nucleic Acids Res* 38, e164. [PubMed: 20601685]
15. Jaganathan K, Kyriazopoulou Panagiotopoulou S, McRae JF, Darbandi SF, Knowles D, Li YI, Kosmicki JA, Arbelaez J, Cui W, Schwartz GB, et al. (2019). Predicting Splicing from Primary Sequence with Deep Learning. *Cell* 176, 535–548 e524. [PubMed: 30661751]

16. Carroll RJ, Bastarache L, and Denny JC (2014). R PheWAS: data analysis and plotting tools for phenome-wide association studies in the R environment. *Bioinformatics* 30, 2375–2376. [PubMed: 24733291]
17. Denny JC, Bastarache L, Ritchie MD, Carroll RJ, Zink R, Mosley JD, Field JR, Pulley JM, Ramirez AH, Bowton E, et al. (2013). Systematic comparison of phenome-wide association study of electronic medical record data and genome-wide association study data. *Nat Biotechnol* 31, 1102–1110. [PubMed: 24270849]
18. Price AL, Kryukov GV, de Bakker PI, Purcell SM, Staples J, Wei LJ, and Sunyaev SR (2010). Pooled association tests for rare variants in exon-resequencing studies. *Am J Hum Genet* 86, 832–838. [PubMed: 20471002]
19. Rothwell PE, Fuccillo MV, Maxeiner S, Hayton SJ, Gokce O, Lim BK, Fowler SC, Malenka RC, and Sudhof TC (2014). Autism-associated neuroligin-3 mutations commonly impair striatal circuits to boost repetitive behaviors. *Cell* 158, 198–212. [PubMed: 24995986]
20. Seibenhener ML, and Wooten MC (2015). Use of the Open Field Maze to measure locomotor and anxiety-like behavior in mice. *J Vis Exp*, e52434.
21. Tucker LB, and McCabe JT (2017). Behavior of Male and Female C57BL/6J Mice Is More Consistent with Repeated Trials in the Elevated Zero Maze than in the Elevated Plus Maze. *Front Behav Neurosci* 11, 13. [PubMed: 28184191]
22. Koch M (1999). The neurobiology of startle. *Prog Neurobiol* 59, 107–128. [PubMed: 10463792]
23. Srikanth P, Lagomarsino VN, Pearse RV, Liao M, Ghosh S, Nehme R, Seyfried N, Eggan K, & Young-Pearse TL (2018). Convergence of independent DISC1 mutations on impaired neurite growth via decreased UNC5D expression. *Translational Psychiatry*, 8(1), 245. [PubMed: 30410030]
24. Saporta MA, Dang V, Volfson D, Zou B, Xie XS, Adebola A, Liem RK, Shy M, and Dimos JT (2015). Axonal Charcot-Marie-Tooth disease patient-derived motor neurons demonstrate disease-specific phenotypes including abnormal electrophysiological properties. *Exp Neurol* 263, 190–199. [PubMed: 25448007]
25. Saredi S, Cauley ES, Ruggieri A, Spivey TM, Ardisson A, Mora M, Moroni I, and Manzini MC (2020). Myopathic changes associated with psychomotor delay and seizures caused by a novel homozygous mutation in TBCK. *Muscle Nerve* 62, 266–271. [PubMed: 32363625]
26. Baar EL, Carbajal KA, Ong IM, and Lamming DW (2016). Sex- and tissue-specific changes in mTOR signaling with age in C57BL/6J mice. *Aging Cell* 15, 155–166. [PubMed: 26695882]
27. de Paula Moreira D, Suzuki AM, e Silva ALT, Varella-Branco E, Meneghetti MCZ, Kobayashi GS, ... & Passos-Bueno MR (2021). Neuroprogenitor cells from patients with TBCK encephalopathy suggest deregulation of early secretory vesicle transport. *Frontiers in cellular neuroscience*, 15.
28. Griesi-Oliveira K, Acab A, Gupta AR, Sunaga DY, Chailangkarn T, Nicol X, ... & Muotri AR (2015). Modeling non-syndromic autism and the impact of TRPC6 disruption in human neurons. *Molecular psychiatry*, 20(11), 1350–1365. [PubMed: 25385366]
29. Marchetto MC, Carromeu C, Acab A, Yu D, Yeo GW, Mu Y, ... & Muotri AR (2010). A model for neural development and treatment of Rett syndrome using human induced pluripotent stem cells. *Cell*, 143(4), 527–539. [PubMed: 21074045]
30. Kulkarni VA, & Firestein BL (2012). The dendritic tree and brain disorders. *Molecular and Cellular Neuroscience*, 50(1), 10–20. [PubMed: 22465229]
31. De Vos KJ, & Hafezparast M (2017). Neurobiology of axonal transport defects in motor neuron diseases: Opportunities for translational research?. *Neurobiology of disease*, 105, 283–299. [PubMed: 28235672]
32. Boecker CA, & Holzbaur EL (2019). Vesicular degradation pathways in neurons: at the crossroads of autophagy and endo-lysosomal degradation. *Current opinion in neurobiology*, 57, 94–101. [PubMed: 30784982]
33. Thangarajh M, Kaat AJ, Bibat G, Mansour J, Summerton K, Gioia A, ... & Wagner KR (2019). The NIH Toolbox for cognitive surveillance in Duchenne muscular dystrophy. *Annals of clinical and translational neurology*, 6(9), 1696–1706. [PubMed: 31472009]

34. Pecker LH, & Naik RP (2018). The current state of sickle cell trait: implications for reproductive and genetic counseling. *Hematology 2014, the American Society of Hematology Education Program Book*, 2018(1), 474–481.
35. Miller AC, Comellas AP, Hornick DB, Stoltz DA, Cavanaugh JE, Gerke AK, ... & Polgreen PM (2020). Cystic fibrosis carriers are at increased risk for a wide range of cystic fibrosis-related conditions. *Proceedings of the National Academy of Sciences*, 117(3), 1621–1627.

Author Manuscript

Author Manuscript

Author Manuscript

Author Manuscript

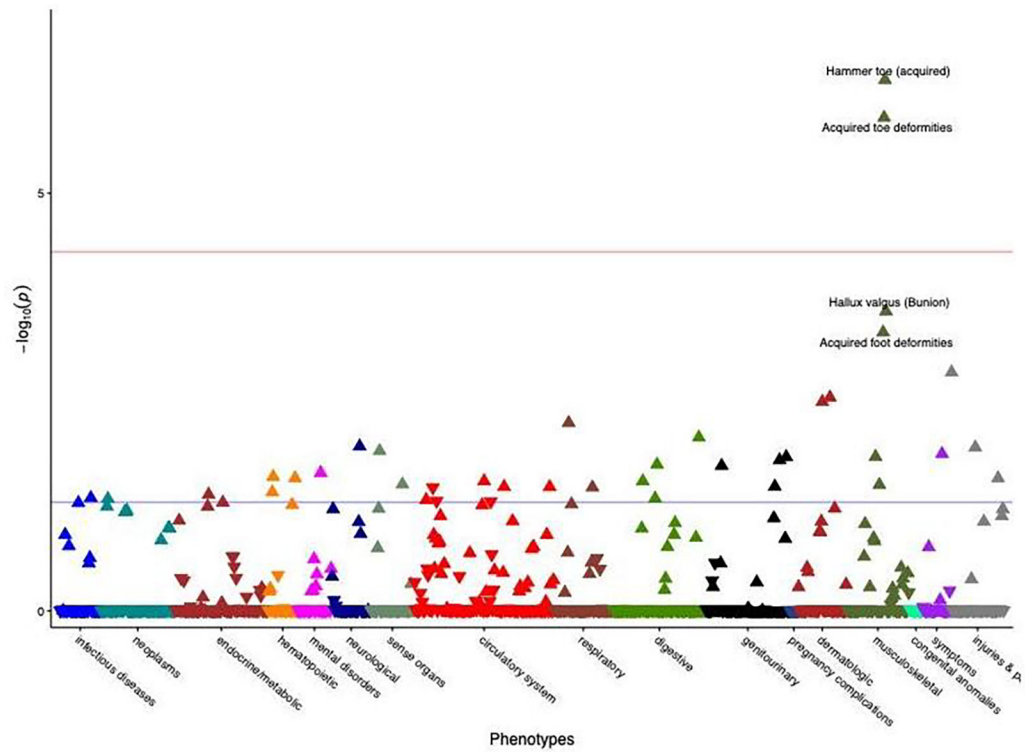


**Figure 1: Gene burden PheWAS of pLOF variants (N=19 heterozygous individuals) in TBCK.** Phecodes are plotted along the x axis to represent the phenome, and the association of the gene burden with each Phecode is plotted along the y axis representing  $-\log_{10}(p)$  value. The red line represents the Bonferroni-corrected significance threshold to adjust for multiple testing ( $p=5E-05$ ), and the blue line represents a nominal significance threshold ( $p=0.05$ ).

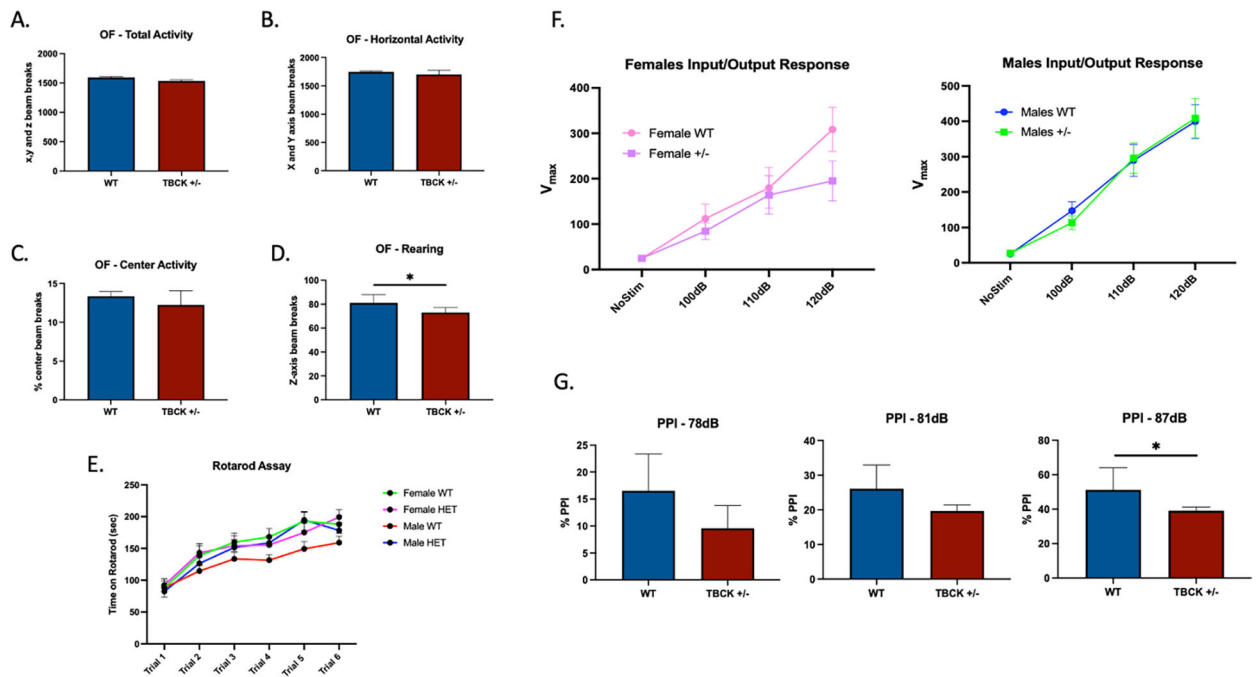


**Figure 2: OF, ASR, and PPI analysis in  $TBCK^{+/-}$  and wild type C57BL/6J animals.**

Animals were habituated for 30min to the procedure room and subsequently underwent open field testing for 10min. Mice were tested for **A.** Open field total activity (WT:  $n=30$  ( $f=14$ ,  $m=16$ ),  $TBCK^{+/-}$ :  $n=28$  ( $f=13$ ,  $m=15$ )), **B.** horizontal activity (WT:  $n=33$  ( $f=16$ ,  $m=17$ ),  $TBCK^{+/-}$ :  $n=32$  ( $f=16$ ,  $m=16$ )), **C.** center activity (WT:  $n=33$  ( $f=16$ ,  $m=17$ ),  $TBCK^{+/-}$ :  $n=32$  ( $f=16$ ,  $m=16$ )), and **D.** rearing (WT:  $n=30$  ( $f=14$ ,  $m=16$ ),  $TBCK^{+/-}$ :  $n=28$  ( $f=13$ ,  $m=15$ )). **E.** rotarod assay ( $n=16-17$ /group), **F.** ASR test measuring the response to 40 ms stimuli of 0 dB, 100 dB, 110 dB, and 120 dB ( $n=16-17$ /group)). **G.** PPI with a 120 dB startle-evoking stimuli delivered alone (no pre-pulse) or preceded by a 20 msec pre-pulse stimuli delivered at three different intensities (WT:  $n=33$  ( $f=16$ ,  $m=17$ ),  $TBCK^{+/-}$ :  $n=32$  ( $f=16$ ,  $m=16$ )).

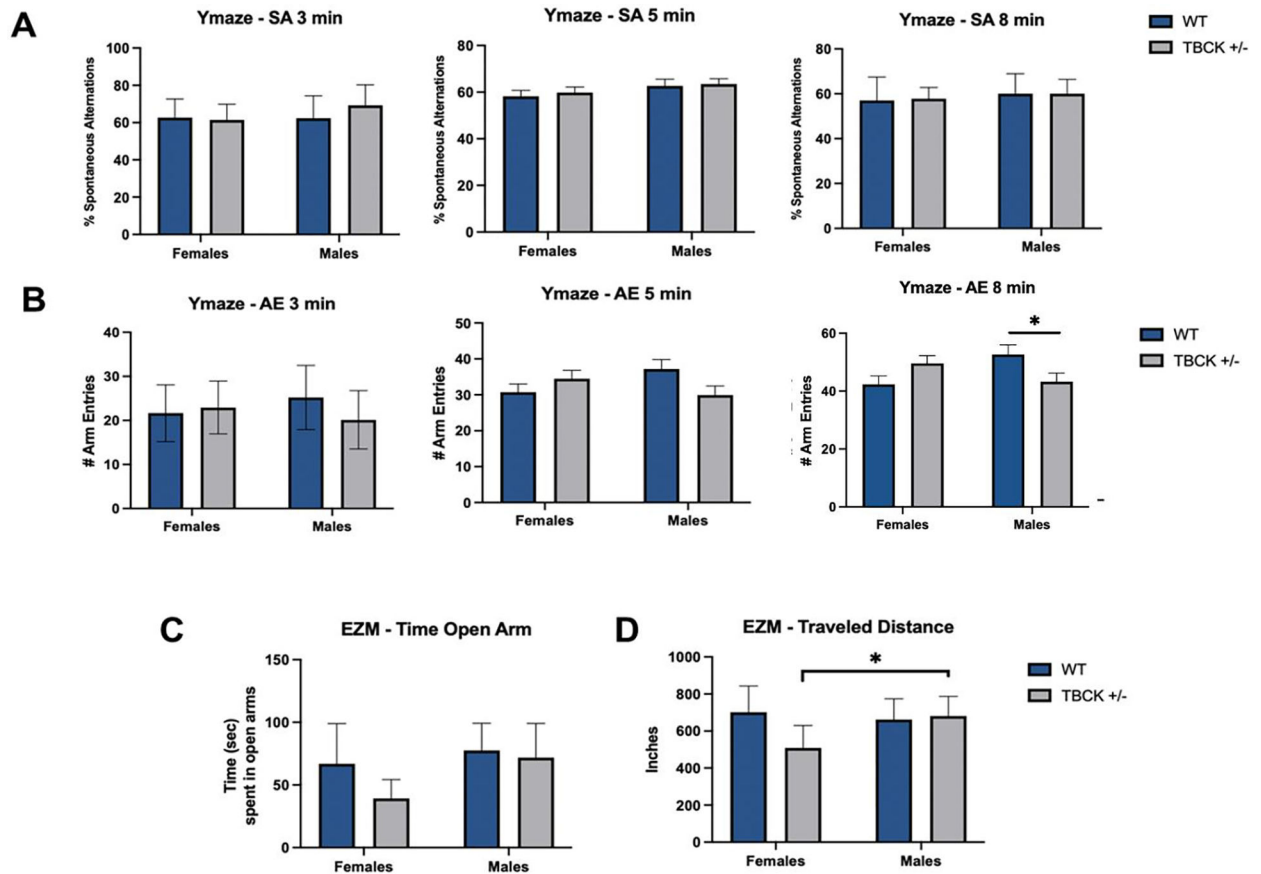


**Figure 3: Y-maze and elevated zero maze behavioral assays in *TBCK*<sup>+/-</sup> and wild type C57BL/6J animals.**

**A.** Spontaneously alternating arm entries in a Y-maze at 3, 5, and 8 minute timepoints ( $n=11-15/\text{group}$ ), **B.** Total arm entries in a Y-maze at 3, 5, and 8 minute timepoints ( $n=11-15/\text{group}$ ), **C.** Time spent in the open areas of the EZM (WT:  $n=7-8/\text{group}$  ( $f=8$ ,  $m=7$ ), TBCK +/-:  $n=3-9/\text{group}$  ( $f=3$ ,  $m=9$ )), **D.** Total distance traveled in the EZM (WT:  $n=7-8/\text{group}$  ( $f=8$ ,  $m=7$ ), TBCK +/-:  $n=3-9/\text{group}$  ( $f=3$ ,  $m=9$ )).

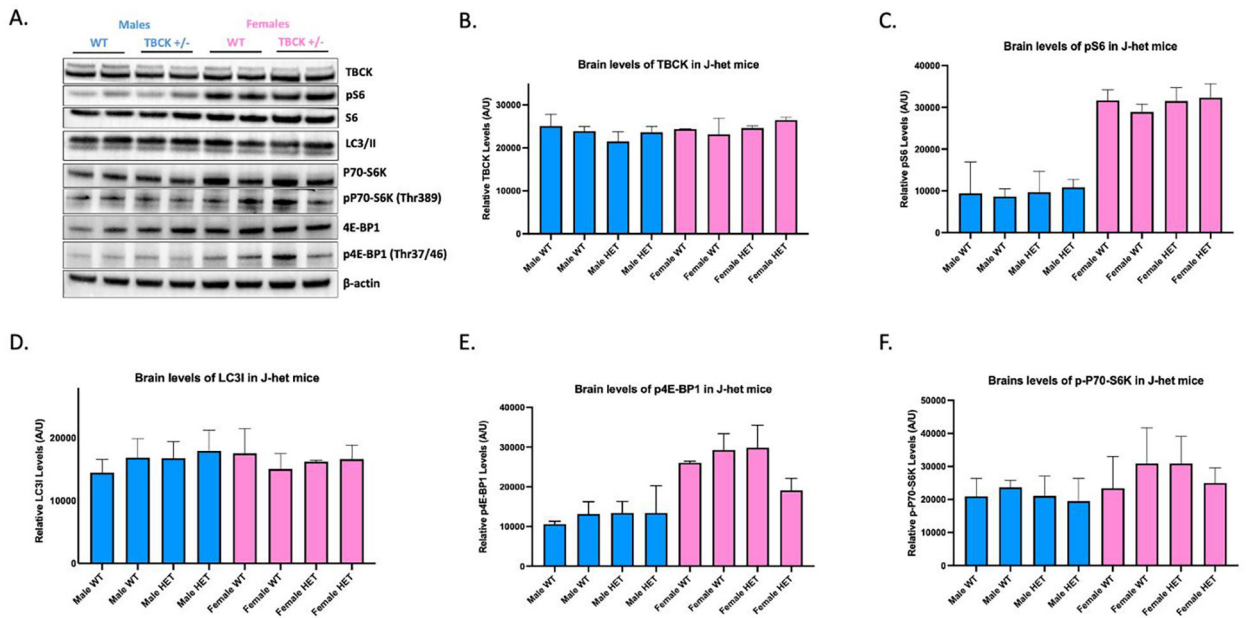


**Figure 4: mTOR signaling is differentially regulated in male vs female mice regardless of genotype.**

Western blotting was performed using TBCK<sup>+/-</sup> and WT mouse total brain lysates.